Applied Physics Express **5** (2012) 063005
DOI: 10.1143/APEX.5.063005

Zero-Field Spin Torque Oscillator Based on Magnetic Tunnel Junctions with a Tilted CoFeB Free Layer

Witold Skowroński*, Tomasz Stobiecki, Jerzy Wrona, Günter Reiss[1], and Sebastiaan van Dijken[2]

Department of Electronics, AGH University of Science and Technology, Al. Mickiewicza 30, 30-059 Kraków, Poland
[1] *Thin Films and Physics of Nanostructures, Bielefeld University, 33615 Bielefeld, Germany*
[2] *NanoSpin, Department of Applied Physics, Aalto University School of Science, P. O. Box 15100, FI-00076 Aalto, Finland*

Received April 6, 2012; accepted May 10, 2012; published online May 28, 2012

Microwave emission from spin torque oscillators based on CoFeB/MgO/CoFeB magnetic tunnel junctions is analyzed with respect to the thickness of the magnetically free electrode. Taking advantage of the ferromagnetic interlayer exchange coupling between the free and reference layers and the perpendicular interface anisotropy of thin CoFeB electrodes on MgO, we demonstrate that large-amplitude oscillations of the tilted CoFeB free layer can be generated in zero applied magnetic field. © 2012 The Japan Society of Applied Physics

Magnetic tunnel junctions (MTJs) consisting of two ferromagnetic electrodes separated by a thin tunnel barrier have drawn significant attention because of their potential use as high-density memory cells[1,2] and microwave electronic components.[3–5] DC currents in such structures can induce a steady-state precession of the magnetic moment due to the interaction between spin-polarized electrons and the local magnetization of the free layer (FL). This spin-transfer-torque (STT) effect[6,7] induces resistance oscillations in the MTJs, which in turn generate an AC voltage signal across the junction in the GHz frequency range. Such STT-based nanometer-scale oscillators could potentially compete with existing LC-tank technologies used in high-frequency electronics. However, one of the main drawbacks of spin torque oscillators (STOs) thus far is the need for an external magnetic field to stabilize their microwave signal. To reduce the external magnetic field in all-metallic spin valve structures, the use of a perpendicular magnetized reference layer (RL) or FL has been explored,[8–11] and the dynamic response as a function of magnetization angle has been numerically simulated.[12] Also, it has been shown that magnetic vortex oscillators can operate in small magnetic fields.[13] Finally, zero-field auto-oscillations of the synthetic ferrimagnet in MTJs have been observed for large tunneling currents that significantly decrease the resistance and tunneling magnetoresistance (TMR).[14]

In this paper, we report on a new approach for the generation of STOs in CoFeB/MgO/CoFeB[15] MTJs without the application of an external magnetic field. Our approach utilizes the perpendicular magnetic anisotropy of the CoFeB/MgO interface to tilt the magnetization of the thin FL layer out-of-the film plane. Together with ferromagnetic interlayer coupling across the thin MgO tunnel barrier, this results in a stable magnetization configuration, which can be excited into persistent microwave-frequency oscillations by STT in zero magnetic field. The ability to operate STOs in this mode opens new routes for the design of spin torque devices without cumbersome magnetic field sources.

The MTJ stack with a CoFeB wedge-shaped electrode was deposited in a Singulus Timaris cluster tool system. The multilayer structure consisted of the following materials (thickness in nm): buffer layers/PtMn (16)/$Co_{70}Fe_{30}$ (2)/Ru (0.9)/$Co_{40}Fe_{40}B_{20}$ (2.3)/MgO (0.85)/$Co_{40}Fe_{40}B_{20}$ (1–2.3)/capping layer. The deposition process was similar to that used in our previous studies.[16,17] After deposition, four different parts of the samples with different FL thicknesses of 1.22, 1.35, 1.57, and 2.3 nm were selected for patterning into nanometer-size pillars. Using a three-step electron beam lithography process, which included ion beam milling, lift-off, and oxide deposition steps, nanopillars with an elliptical cross section of $250 \times 150\,\text{nm}^2$ were fabricated. The pillars were etched to the PtMn layer. To ensure good RF performance, the overlap between the top and bottom leads was limited to about $4\,\mu\text{m}^2$, which resulted in a capacitance of less than 1×10^{-14} F. The DC measurements were conducted at room temperature with a magnetic field applied in the sample plane. The high-frequency measurements were carried out using an Agilent N9030A spectrum analyzer with a built-in preamplifier. The MTJ bonded to a high-frequency chip carrier was connected to a bias tee. The DC signal from a sourcemeter was fed to the sample through the inductive connector of the bias tee and the spectrum was measured at the capacitive connector. In this paper, a positive voltage denotes electrons tunneling from the bottom RL to the top FL. This current direction favors a parallel alignment of the FL and RL magnetizations due to spin-transfer torque.

Figure 1 shows TMR loops for all samples, with the field applied along the in-plane easy axis of the MTJ. The shape of the TMR curves changes as a function of FL thickness. For 2.3 nm CoFeB, the FL switches abruptly, indicating an in-plane alignment of the FL magnetization. The TMR of the junction with the thinnest FL, on the other hand, varies linearly with applied magnetic field. In this case, the magnetization of the FL is oriented out-of-plane in remanence and the application of a magnetic field coherently rotates the magnetization towards the film plane. The responses of the samples with 1.35 and 1.57 nm FLs are attributed to an intermediate configuration whereby the average magnetization angle of the CoFeB FL is tilted out of the film plane. The out-of-plane tilt of the FL originates from a perpendicular anisotropy effect at the MgO/CoFeB interface.[18,19] The competition between this interface anisotropy and the in-plane shape anisotropy results in a spin reorientation transition with increasing FL thickness. The thickness range for this transition in our experiments (∼1.2–2.3 nm) agrees well with those in the literature.[18–20] Table I shows the transport properties of the MTJs. The average tilt angle of the FL magnetization in zero magnetic field was estimated from the shape of the TMR curves. The observed decrease in the level of the TMR effect with decreasing FL thickness is

---

*E-mail address: skowron@agh.edu.pl

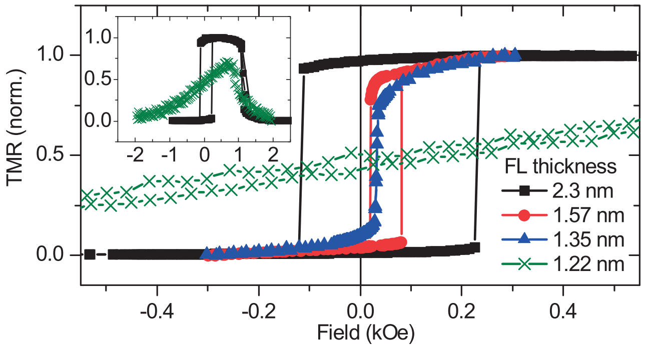

Fig. 1. Normalized TMR vs magnetic field curves for junctions with different FL thicknesses measured with a bias voltage of $V_b = 10\,\text{mV}$. The inset shows the same data for the samples with 1.22 and 2.3 nm FLs for larger applied magnetic fields. The abrupt switching of the 2.3 nm FL indicates an in-plane alignment of the CoFeB magnetization, whereas the linear response of the 1.22 nm FL demonstrates a hard in-plane magnetization axis. For the MTJ with a 1.22 nm FL, a full AP state is not reached, because the RL flips at 0.8 kOe. The TMR for this sample is normalized to the extrapolated AP resistance value.

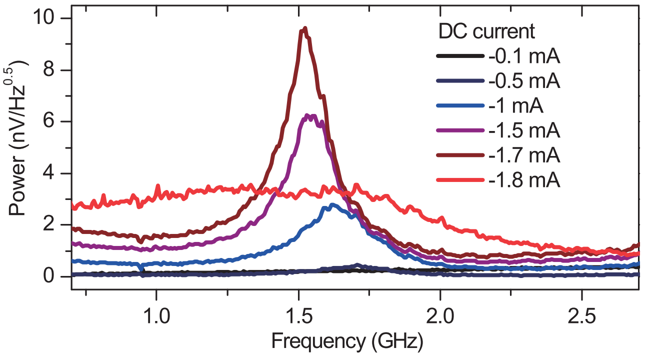

Fig. 2. STO spectra of MTJ with a 1.57 nm FL measured in zero external magnetic field for different negative tunneling currents.

Table I. Summary of MTJ parameters. The STO integrated power was calculated from the power density spectra curves measured with a current of $I_b = -1\,\text{mA}$. The critical current is defined as the current necessary to switch the magnetization from the P state to the AP state in zero external magnetic field.

Free layer thickness (nm)	TMR ratio (%)	Resistance parallel (Ω)	Average tilt angle (deg)	Integrated power (pW)	Critical current (mA)
1.22	8	102	84	—	—
1.35	50	120	43	411	−0.95
1.57	100	110	26	19.3	−1.8
2.3	120	130	4	2.4	−2.4

partly caused by the out-of-plane tilt of the FL magnetization [abrupt switching between parallel (P) and antiparallel (AP) magnetization states is no longer achieved for a 1.22 nm FL] and it is further reduced by a decrease in the spin polarization of ultrathin CoFeB films.[21)] Another important parameter for obtaining zero-field spin torque oscillations is the interlayer coupling between the two CoFeB electrodes. In our junctions, the coupling between the FL and the RL is ferromagnetic as evidenced by the positive field shift in the TMR curves in Fig. 1. The ferromagnetic interlayer coupling, whose origin is analyzed in detail in refs. 16 and 22, stabilizes the low resistance state of the MTJs in zero magnetic field.

In quasi-static transport measurements, the samples with a FL thickness of 1.35–2.3 nm show a clear current-induced magnetization switching for relatively long current pulses of 10 ms. The absolute switching current that is required to switch the MTJ from a low resistance state to a high resistance state in zero applied magnetic field decreases in thin FLs (Table I). This effect is most likely caused by an increase in FL tilt angle and a reduction in FL magnetic moment. Abrupt switching does not occur in junctions with a 1.22 nm FL and, consequently, quasi-static current-induced effects are absent.

Because the switching voltage is much smaller than the breakdown voltage, steady-state precessions can be induced without destroying the MTJ. A selection of STO spectra for a sample with a 1.57 nm FL is shown in Fig. 2. No magnetic field was applied during these measurements. For this MTJ, the perpendicular anisotropy of the CoFeB/MgO interface tilts the magnetization of the FL out of the film plane, while its in-plane component remains parallel to the magnetization of the RL and, thus, a relatively low resistance state is obtained (Fig. 1). Under these conditions, the excitation of steady-state precessions requires only a small DC current. An increase in negative tunneling current that favors the AP state (electrons flowing from the FL to the RL) increases the amplitude of the oscillations to more than $9\,\text{nV/Hz}^{1/2}$ (0.14 nW power) at 1.5 GHz and −1.7 mA. Here, corrections due to impedance mismatch were taken into account.[3)] A further increase in negative DC current switches the MTJ to the high-resistance AP state, for which the STO peak is broader and less intense.

The peak frequency (f_0) and its evolution with magnetic field strength are consistent with the excitation of microwave-frequency oscillation in the CoFeB FL of our MTJs. This is also confirmed by simulations that take appropriate magnetic anisotropy values into account. STOs of the synthetic ferrimagnetic RL, which are expected to occur at higher frequencies, are not observed in our experiments.[23)] We also note that the resistance and TMR of the junctions do not change during microwave excitation in zero magnetic field.

Figure 3 shows the STO amplitudes, f_0, and linewidth (Δf) versus DC tunneling current in zero external magnetic field. Clearly, the oscillation amplitude increases with decreasing FL thickness. Larger amplitudes are thus obtained when the magnetization of the CoFeB FL is tilted out of the film plane. Moreover, for samples with FL thicknesses of 1.35 and 1.57 nm, a pronounced asymmetry is observed with respect to the polarity of the tunneling current. For these samples, the oscillations are more powerful for negative currents favoring the AP state than for positive currents favoring the P state. This asymmetry is expected because the MTJ is in a near P state and, hence, the spin torque effect tends to destabilize the FL magnetization more for negative polarity. For the MTJ with a FL thickness of 2.3 nm, the oscillation amplitude is smaller and symmetric with respect to the polarity of the current, which is reminiscent of thermally excited resonances.[5)]

f_0 in zero applied magnetic field increases with increasing FL thickness as shown in Fig. 3(b). This evolution is explained by an increase in the in-plane magnetic anisotropy of

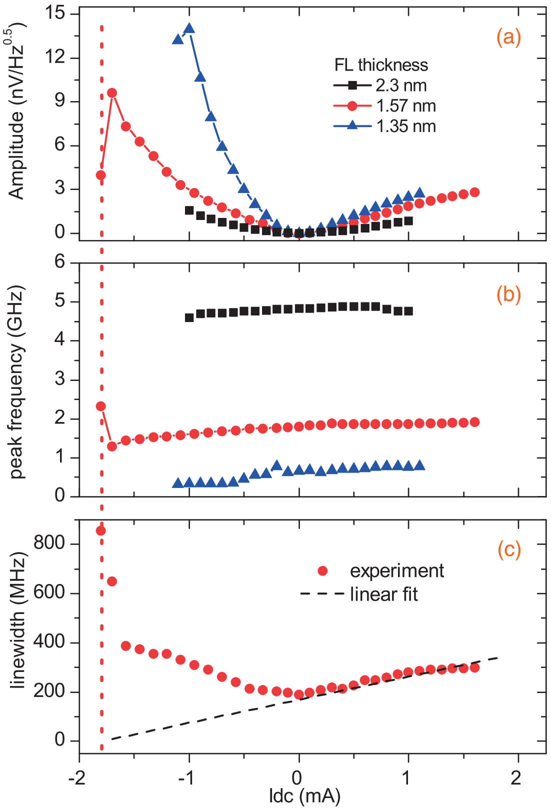

Fig. 3. DC bias current dependence of the STO amplitude (a), peak frequency f_0 (b), and linewidth Δf (sample 1.57 only) (c). No magnetic field was applied during the measurements. The dashed line in (c) represents a linear fit to the experimental data for positive I_{dc}. Near the switching current (dotted line), both f_0 and Δf increase.

the FL, which results in smaller precession trajectories and larger f_0. We note that a sample-to-sample distribution in both oscillation amplitude and frequency is observed, due to the size and shape distribution after nanolithography processing, however, the overall tendency is retained. For the MTJ with a 1.22 nm FL, we were not able to observe any oscillations in the measured bandwidth even with magnetic fields of up to 0.25 T applied parallel or perpendicular to the sample plane.

The dependence of oscillation linewidth on DC tunneling current can be expressed as

$$\Delta f = \frac{\sigma}{2\pi}(I_{\mathrm{c0}} - I_{\mathrm{dc}}), \tag{1}$$

where σ is the spin polarization efficiency and I_{c0} is the critical switching current.[24] Extrapolation of Δf at the damping side (when the MTJ is in a near P state and the current direction favors the P state) to zero frequency gives an estimation of the switching current (dotted line in Fig. 3) of about -1.7 mA, which is in good agreement with the value of -1.8 mA from quasi-static transport measurements (Table I). Moreover, abrupt changes in f_0 and Δf observed near the switching threshold also indicate a transition from steady-state precessions to current-induced magnetization switching.

In summary, we have demonstrated that CoFeB/MgO/CoFeB STOs can produce microwave signals in zero external magnetic field. Due to ferromagnetic interlayer exchange coupling in our MTJs, the STOs are in a low-resistance state in zero field. The perpendicular interface anisotropy of the CoFeB FL on top of the MgO tunnel barrier tilts the FL magnetization out of the film plane and this stabilizes steady-state precessions in small DC tunneling currents. We conclude that by taking advantage of the coupling mechanisms in MTJs and the perpendicular anisotropy of the MgO/CoFeB interface, the performance of STOs can be enhanced without the need of an external magnetic field.

Acknowledgments The authors would like to thank Singulus Technologies AG for consultation and technical help with the preparation of MgO-based MTJs. T.S. and W.S. acknowledge the Foundation for Polish Science MPD Programme cofinanced by the EU European Regional Development Fund, Polish Ministry of Science and Higher Education and National Science Center grants (IP 2010037970 and NN 515544538). G.R. acknowledges financial support from the Deutsche Forschungsgemeinschaft (RE 1052/22). S.V.D. acknowledges financial support from the Academy of Finland (SA 127731).

---

1) Y. Huai, F. Albert, P. Nguyen, M. Pakala, and T. Valet: Appl. Phys. Lett. **84** (2004) 3118.
2) R. Takemura, T. Kawahara, K. Miura, H. Yamamoto, J. Hayakawa, N. Matsuzaki, K. Ono, M. Yamanouchi, K. Ito, H. Takahashi, S. Ikeda, H. Hasegawa, H. Matsuoka, and H. Ohno: IEEE J. Solid-State Circuits **45** (2010) 869.
3) S. I. Kiselev, J. C. Sankey, I. N. Krivorotov, N. C. Emley, R. J. Schoelkopf, R. A. Buhrman, and D. C. Ralph: Nature **425** (2003) 380.
4) W. Rippard, M. Pufall, S. Kaka, S. Russek, and T. Silva: Phys. Rev. Lett. **92** (2004) 027201.
5) A. M. Deac, A. Fukushima, H. Kubota, H. Maehara, Y. Suzuki, S. Yuasa, Y. Nagamine, K. Tsunekawa, D. D. Djayaprawira, and N. Watanabe: Nat. Phys. **4** (2008) 803.
6) J. C. Slonczewski: J. Magn. Magn. Mater. **159** (1996) L1.
7) L. Berger: Phys. Rev. B **54** (1996) 9353.
8) O. Boulle, V. Cros, J. Grollier, L. G. Pereira, C. Deranlot, F. Petroff, G. Faini, J. Barnaś, and A. Fert: Nat. Phys. **3** (2007) 492.
9) D. Houssameddine, U. Ebels, B. Delaët, B. Rodmacq, I. Firastrau, F. Ponthenier, M. Brunet, C. Thirion, J.-P. Michel, L. Prejbeanu-Buda, M.-C. Cyrille, O. Redon, and B. Dieny: Nat. Mater. **6** (2007) 447.
10) W. H. Rippard, A. M. Deac, M. R. Pufall, J. M. Shaw, M. W. Keller, S. E. Russek, and C. Serpico: Phys. Rev. B **81** (2010) 014426.
11) A. Mourachkine, O. V. Yazyev, C. Ducati, and J.-Ph. Ansermet: Nano Lett. **8** (2008) 3683.
12) Y. Zhou, S. Bonetti, C. L. Zha, and J. Åkerman: New J. Phys. **11** (2009) 103028.
13) V. S. Pribiag, I. N. Krivorotov, G. D. Fuchs, P. M. Braganca, O. Ozatay, J. C. Sankey, D. C. Ralph, and R. A. Buhrman: Nat. Phys. **3** (2007) 498.
14) T. Devolder, L. Bianchini, J.-V. Kim, P. Crozat, C. Chappert, S. Cornelissen, M. Op de Beeck, and L. Lagae: J. Appl. Phys. **106** (2009) 103921.
15) D. D. Djayaprawira, K. Tsunekawa, M. Nagai, H. Maehara, S. Yamagata, N. Watanabe, S. Yuasa, Y. Suzuki, and K. Ando: Appl. Phys. Lett. **86** (2005) 092502.
16) W. Skowroński, T. Stobiecki, J. Wrona, K. Rott, A. Thomas, G. Reiss, and S. van Dijken: J. Appl. Phys. **107** (2010) 093917.
17) J. Wrona, J. Langer, B. Ocker, W. Maass, J. Kanak, T. Stobiecki, and W. Powroźnik: J. Phys.: Conf. Ser. **200** (2010) 052032.
18) S. Yakata, H. Kubota, Y. Suzuki, K. Yakushiji, A. Fukushima, S. Yuasa, and K. Ando: J. Appl. Phys. **105** (2009) 07D131.
19) S. Ikeda, K. Miura, H. Yamamoto, K. Mizunuma, H. D. Gan, M. Endo, S. Kanai, J. Hayakawa, F. Matsukura, and H. Ohno: Nat. Mater. **9** (2010) 721.
20) P. Wiśniowski, J. M. Almeida, S. Cardoso, N. P. Barradas, and P. P. Freitas: J. Appl. Phys. **103** (2008) 07A910.
21) J. J. Sun and P. P. Freitas: J. Appl. Phys. **85** (1999) 5264.
22) S. Serrano-Guisan, W. Skowroński, J. Wrona, N. Liebing, M. Czapkiewicz, T. Stobiecki, G. Reiss, and H. W. Schumacher: J. Appl. Phys. **110** (2011) 023906.
23) S. Cornelissen, L. Bianchini, T. Devolder, J.-V. Kim, W. Van Roy, L. Lagae, and C. Chappert: Phys. Rev. B **81** (2010) 144408.
24) T. Wada, T. Yamane, T. Seki, T. Nozaki, Y. Suzuki, H. Kubota, A. Fukushima, S. Yuasa, H. Maehara, Y. Nagamine, K. Tsunekawa, D. D. Djayaprawira, and N. Watanabe: Phys. Rev. B **81** (2010) 104410.